

Non-Markovian dynamics in continuous measurement of a solid-state charge qubit

JunYan Luo,* Lun-Wu Zhu, Xiao-Ling He, Bensheng Yun, and Shiping Ruan
School of Science, Zhejiang University of Science and Technology, Hangzhou 310023, China

HuJun Jiao
Department of Physics, Shanxi University, Taiyuan, Shanxi 030006, China

Continuous measurement of a quantum two-level system (qubit) by mesoscopic charge detectors has attracted wide attention in the community of solid-state quantum computation. In this work, we revisit the measurement of a charge qubit by a quantum point contact, with particular attention paid to the unique non-Markovian measurement characteristics. The finite-frequency-support feature due to non-Markovian correlation leads to a remarkable suppression of the pedestal in noise spectrum, which results in a drastic violation of the Korotkov-Averin bound, the upper limit of the single-to-noise ratio imposed quantum mechanically on linear detectors. For a large measurement voltage and bandwidth, the non-Markovian effect gives rise to a complete inhibition of coherent jumps (quantum Zeno effect), as identified by the telegraph noise peaks in the spectrum.

PACS numbers: 03.65.Ta, 72.70.+m, 03.65.Yz, 03.65.Xp

I. INTRODUCTION

The dynamics of quantum measurement is an essential element in the rapidly developing field of quantum computing [1, 2]. So far, various mesoscopic devices have been proposed to monitor the continuous evolution of a charge qubit. Among them, especially interesting ones are electrometers, such as single electron transistor (SET) [3–10] and quantum point contact (QPC) [11–15], whose conductance depends on the charge state of a nearby qubit. From the readout of the detectors, correlations in transport of all orders can be accessed by analyzing the full spectrum of counting statistics [16].

Evaluation of the shot noise and higher cumulants in FCS are often studied in the wide-band limit (WBL) and under Markovian approximation [17–26]. The WBL neglects the energy-dependent densities of states in the electrodes. The Markovian approximation assumes the correlation time in the electrodes is much shorter than that in the reduced system. Yet, these approximations may not be always true in realistic devices. Recently, memory effects of environment on the noise characteristics were investigated, with important non-Markovian correlations being revealed [27–29]. Flindt et al [30] and Aguado et al [31] studied the noise spectrum of a qubit under transport, with a non-Markovian treatment of the phonon bath. The non-Markovian correlations of electrodes were investigated in the context of a transport single quantum dot [32, 33], and a nanomechanical resonator measured by a QPC [34], in which considerable difference in dynamics between the non-Markovian and Markovian cases was identified.

The aim of this work is to study the unique non-Markovian dynamics in continuous measurement of a

charge qubit by a QPC. Our calculation is based on a time nonlocal generalized quantum master equation approach [32, 35], which is capable of treating properly the energy exchange between the qubit and detector. The finite-frequency-support feature due to non-Markovian correlation results in a remarkable suppression of the pedestal of the noise spectrum, which eventually leads to a drastic violation of the Korotkov-Averin bound, the upper limit of the signal-to-noise ratio imposed quantum mechanically on linear detectors [36]. Previous studies in the Markovian regime showed that resonant peaks in the noise spectrum were observed in the wide band and large bias limit, due to electron coherent jumps [37, 38]. Yet, we find here that strong non-Markovian correlation results in complete incoherent jumps between the two states (quantum Zeno effect), as indicated by telegraph noise peaks in the spectrum. An increase in temperature induces complex spontaneous qubit relaxation and dephasing. For a narrow bandwidth and large voltage, coherent oscillation is robust over a wide range of temperatures. Spontaneous qubit relaxation causes delocalization of the electron, and thus lower the incoherent peak. Yet, different from the results reported in Ref. [39], the spontaneous relaxation observed here can not eliminate the Zeno effect completely.

This paper is organized as follows. We begin in Sec. II with the model set-up of a charge qubit under the continuous measurement by a QPC. We then present in Sec. III the time nonlocal generalized quantum master equation, unraveled into its “ N ”-resolved components. Numerical results and discussions are presented in Sec. IV, and it is then followed by the conclusion in Sec. V.

II. MODEL DESCRIPTION

The system under investigation is schematically shown in Fig. 1. The qubit is represented by an electron tunneling between two coherently coupled quantum dots. A

*Electronic address: jylo@zust.edu.cn

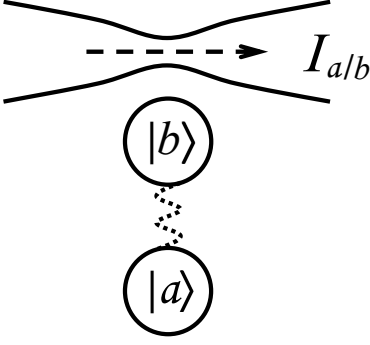


FIG. 1: Schematic setup of a solid-state charge qubit measured continuously by a quantum point contact.

nearby QPC serves as a charge detector to continuously monitor the the position of the electron. The Hamiltonian of the entire system is of $H_T = H_{\text{qu}} + H_D + H'$, with the qubit, QPC detector, and their coupling parts being modeled respectively by

$$H_{\text{qu}} = \frac{1}{2}\epsilon\sigma_z + \Omega\sigma_x, \quad (1a)$$

$$H_D = \sum_{k \in L} \epsilon_k \hat{c}_k^\dagger \hat{c}_k + \sum_{q \in R} \epsilon_q \hat{c}_q^\dagger \hat{c}_q, \quad (1b)$$

$$H' = \sum_{s=a,b} \sum_{k,q} t_{kq}^s \hat{c}_k^\dagger \hat{c}_q \cdot |s\rangle\langle s| + \text{H.c.}, \quad (1c)$$

where the pseudospin operators are $\sigma_z \equiv |a\rangle\langle a| - |b\rangle\langle b|$ and $\sigma_x \equiv |a\rangle\langle b| + |b\rangle\langle a|$, respectively. The amplitude t_{kq}^s of electron tunneling through two reservoirs ($\alpha = L$ and R) of the QPC depends explicitly on the qubit state $|s\rangle$ ($s = a$ or b). By denoting $Q_s \equiv |s\rangle\langle s|$, the qubit-QPC detector coupling in the H_D -interaction picture reads as $H'(t) = \sum_s [\hat{f}_s(t) + \hat{f}_s^\dagger(t)] \cdot Q_s$, with $\hat{f}_s(t) \equiv e^{iH_D t} (\sum_{k,q} t_{kq}^s \hat{c}_k^\dagger \hat{c}_q) e^{-iH_D t}$. The effects of the stochastic QPC reservoirs on measurement are characterized by the bath correlation functions $\tilde{C}_{ss'}^{(+)}(t-\tau) \equiv \langle \hat{f}_s^\dagger(t) \hat{f}_{s'}(\tau) \rangle$ and $\tilde{C}_{ss'}^{(-)}(t-\tau) \equiv \langle \hat{f}_s(t) \hat{f}_{s'}^\dagger(\tau) \rangle$. By introducing the reservoir spectral density function

$$J_{ss'}(\omega, \omega') = \sum_{k,q} t_{kq}^s t_{kq}^{s'} \delta(\omega - \epsilon_k) \delta(\omega' - \epsilon_q), \quad (2)$$

these QPC coupling correlation functions can be reexpressed as

$$\tilde{C}_{ss'}^{(\pm)}(t) = \iint d\omega d\omega' J_{ss'}(\omega, \omega') f_L^{(\pm)}(\omega) f_R^{(\mp)}(\omega') e^{\pm i(\omega - \omega')t}, \quad (3)$$

where $f_\alpha^{(\pm)}(\omega) = \{1 + e^{\pm \beta(\omega - \mu_\alpha)}\}^{-1}$ are related to the Fermi function of the electrode α , and $\beta = (k_B T)^{-1}$ is the inverse temperature. Throughout this work, we set $\mu_L^{\text{eq}} = \mu_R^{\text{eq}} = 0$ for the equilibrium chemical potentials (or Fermi energies) of the QPC reservoirs in the absence

of applied bias voltage, and $\hbar = e = 1$ for the Planck constant and electron charge.

The Laplace transform of the correlation function used later is defined by

$$\mathcal{Q}_{ss'}^{(\pm)}(z) \equiv \int_0^\infty dt \tilde{C}_{ss'}^{(\pm)}(t) e^{-zt}. \quad (4)$$

In the limit $z \rightarrow i\omega$, it is further simplified to

$$\mathcal{Q}_{ss'}^{(\pm)}(z)|_{z \rightarrow i\omega} = C_{ss'}^{(\pm)}(\omega) + iD_{ss'}^{(\pm)}(\omega). \quad (5)$$

The coupling spectrum function here is defined as

$$C_{ss'}^{(\pm)}(\omega) \equiv \int_{-\infty}^\infty dt \tilde{C}_{ss'}^{(\pm)}(t) e^{-i\omega t}. \quad (6)$$

which is associated with particle transfer processes, with interactions between the qubit and QPC being properly accounted for. The dispersion function $D_{ss'}^{(\pm)}(\omega)$ can then be evaluated via the Kramers-Kronig relation,

$$D_{ss'}^{(\pm)}(\omega) = \frac{1}{\pi} \mathcal{P} \int_{-\infty}^\infty d\omega' \frac{C_{ss'}^{(\pm)}(\omega')}{\omega - \omega'}, \quad (7)$$

where \mathcal{P} stands for Cauchy's principal value. Physically, the dispersion accounts for the coupling-induced energy renormalization of the internal energies [40–43].

In order to account for finite bandwidth of the QPC detector, we introduce a single Lorentzian to model the band structure. Real spectral density has a complicated structure, which can be parameterized via the technique of spectral decomposition [44, 45]. This complexity, however, will only modify details of the results, but not the qualitative picture. For the sake of constructing analytical results, we assume a simple Lorentzian function centered at the Fermi energy for the spectral density Eq. (2). Moreover, the bias voltage is conventionally described by a relative shift of the entire energy-bands, thus the centers of the Lorentzian functions would fix at the Fermi levels. Without loss of generality, we assume [38]

$$J_{ss'}(\omega, \omega') = \chi_s \chi_{s'} \frac{\Gamma_L^0 w^2}{(\omega - \mu_L)^2 + w^2} \cdot \frac{\Gamma_R^0 w^2}{(\omega' - \mu_R)^2 + w^2}. \quad (8)$$

The asymmetric qubit-QPC coupling parameter is of $\chi_a > \chi_b$, as inferred from Fig.1. The coupling spectrum function of Eq. (6) can be evaluated as $C_{ss'}^{(\pm)}(\omega) = \chi_s \chi_{s'} C^{(\pm)}(\omega)$, with

$$C^{(\pm)}(\omega) = \frac{\eta g(x)}{1 - e^{\beta x}} \left[\frac{w^2}{x} \{ \phi(0) - \phi(x) \} - \frac{w}{2} \varphi(x) \right]_{x=\omega \pm V}. \quad (9)$$

Here, $\eta = 2\pi \Gamma_L^0 \Gamma_R^0$, $g(x) = 4w^2/(x^2 + 4w^2)$, and $V = \mu_L - \mu_R$ the applied voltage on the QPC detector; $\phi(x)$ and $\varphi(x)$ denote the real and imaginary parts of the digamma function $\Psi(\frac{1}{2} + \beta \frac{w+ix}{2\pi})$, respectively. Knowing the spectral function, the dispersion function $D_{ss'}^{(\pm)}(\omega) =$

$\chi_s \chi_{s'} D^{(\pm)}(\omega)$ can be obtained via the Kramers–Kronig relation. It is worth mentioning here that the present spectrum functions satisfy the detailed-balance relation, i.e. $C^{(+)}(\omega) = e^{-\beta(\omega+V)} C^{(-)}(-\omega)$, which means that our approach properly accounts for the energy exchange between the qubit and the detector during measurement.

III. PARTICLE-NUMBER-RESOLVED MASTER EQUATION

The non-Markovian dynamics of the reduced system is described by a time nonlocal quantum master equation [35]. To achieve the description of the output characteristics, we unravel the reduced density matrix $\rho(t)$ into components $\rho^{(N)}(t)$, in which “ N ” is the number of electrons passing through the QPC during the time span $[0, t]$. The resultant time nonlocal “ N ”-resolved quantum master equation reads [5, 30–33]

$$\dot{\rho}^{(N)}(t) = -i\mathcal{L}\rho^{(N)}(t) - \int_0^t d\tau \left\{ \Pi_0(t-\tau)\rho^{(N)}(\tau) - \sum_{\pm} \Pi_{\pm}(t-\tau)\rho^{(N\pm 1)}(\tau) \right\} + \varrho^{(N)}(t), \quad (10)$$

Here, the first term $\mathcal{L}(\cdots) \equiv [H_{\text{qu}}, (\cdots)]$ is the qubit Liouvillian. The memory kernels Π_0 and Π_{\pm} describes the influence of the QPC detector on the dynamics of the qubit, while the inhomogeneity $\varrho^{(N)}$ accounts for initial correlations between qubit and detector.

We assume that the system evolves from $t_0 = -\infty$, such that the electronic occupation probabilities at $t = 0$, where electron counting begins, have reached the stationary state, i.e., $\rho^{(N)}(t = 0) = \delta_{N,0}\rho^{\text{st}}$, with $\rho^{\text{st}} = \rho(t \rightarrow \infty)$. For this model, the “ N ”-resolved quantum master equation in the Laplace domain reads

$$z\tilde{\rho}^{(N)}(z) - \delta_{N,0}\rho^{\text{st}} = -i\mathcal{L}\tilde{\rho}^{(N)}(z) - \left\{ \tilde{\Pi}_0(z)\tilde{\rho}^{(N)}(z) - \tilde{\Pi}_+(z)\tilde{\rho}^{(N+1)}(z) - \tilde{\Pi}_-(z)\tilde{\rho}^{(N-1)}(z) \right\} + \tilde{\varrho}^{(N)}(z), \quad (11)$$

where

$$\tilde{\Pi}_0(z)(\cdots) = \sum_{ss'} \left\{ Q_s \mathcal{Q}_{ss'}(z + i\mathcal{L})Q_{s'}(\cdots) + \mathcal{Q}_{ss'}(z^* - i\mathcal{L})(\cdots)Q_{s'}Q_s \right\}, \quad (12a)$$

$$\tilde{\Pi}_{\pm}(z)(\cdots) = \sum_{ss'} \left\{ \mathcal{Q}_{ss'}^{(\pm)}(z + i\mathcal{L})Q_{s'}(\cdots)Q_s + Q_s \mathcal{Q}_{ss'}^{(\pm)}(z^* - i\mathcal{L})(\cdots)Q_{s'} \right\}, \quad (12b)$$

with $\mathcal{Q}_{ss'} = \mathcal{Q}_{ss'}^{(+)} + \mathcal{Q}_{ss'}^{(-)}$. Note here due to finite bandwidth of the QPC detector and quasistep feature in the Fermi functions in Eq. (3), $\mathcal{Q}_{ss'}^{(\pm)}$ decays exponentially when ω goes beyond the bandwidth. As a result, the resolvent of the kernels $\tilde{\Pi}_0(z)$ and $\tilde{\Pi}_{\pm}(z)$ vanish in the limit $\omega \rightarrow \infty$. The finite-frequency-support feature of $\mathcal{Q}_{ss'}^{(\pm)}$ will have important impact on the measurement effectiveness of the QPC detector.

The unraveling of the density matrix in Eq. (10) allows us to evaluate the probability distribution for the number of transferred charge $P(N, t) = \text{tr}\{\rho^{(N)}(t)\}$, where the trace is over the reduced system degrees of freedom. All the cumulants of the current distribution can be obtained, consisting a spectrum of full counting statistics. For instance, the first cumulant is directly related to the average current through the QPC, $I(t) = \sum_N N \dot{P}(N, t)$.

By using of Eq. (10), it is given by

$$I(t) = \int_0^t d\tau \text{tr}\{[\Pi_-(t-\tau) - \Pi_+(t-\tau)]\rho(\tau)\}. \quad (13)$$

The stationary current thus reads

$$\bar{I} \equiv I(t \rightarrow \infty) = \text{tr}\{J_-(z)\rho^{\text{st}}\}, \quad (14)$$

with

$$J_{\pm}(z) = \tilde{\Pi}_-(z) \pm \tilde{\Pi}_+(z). \quad (15)$$

The second cumulant of the current distribution corresponds to the shot noise. To study the finite-frequency spectrum, we employ the MacDonald’s formula [46]

$$S(\omega) = 2\omega \int_0^{\infty} dt \sin(\omega t) \frac{d}{dt} [\langle N^2(t) \rangle - (\bar{I}t)^2], \quad (16)$$

with $\langle N^2(t) \rangle \equiv \sum_N N^2 P(N, t)$. By utilizing Eq. (10)), the shot noise is simplified to

$$S(\omega) = 2\omega \text{Im}[\text{tr}\{2J_-(z)\tilde{N}(z) + J_+(z)\tilde{\rho}^{\text{st}}(z)\}]|_{z \rightarrow i\omega}, \quad (17)$$

where $\tilde{\rho}^{\text{st}}(z) = \rho^{\text{st}}/z$, and $\tilde{N}(z)$ the counterpart of $N(t) = \sum_N N \rho^{(N)}(t)$ in the Laplace domain. It can be solved from the following algebraic equation

$$z\tilde{N}(z) = -i\mathcal{L}\tilde{N}(z) - \tilde{\Pi}(z)\tilde{N}(z) + J_-(z)\tilde{\rho}^{\text{st}}(z), \quad (18)$$

where $\tilde{\Pi}(z) \equiv \tilde{\Pi}_0(z) - \tilde{\Pi}_+(z) - \tilde{\Pi}_-(z)$.

IV. RESULTS AND DISCUSSIONS

In continuous weak measurement of a qubit, one of the most important signatures is the resonance peak at frequencies around the hybridization energy $\Delta = \sqrt{\epsilon^2 + (2\Omega)^2}$. The basic physics of the measurement process is a trade-off between acquisition of information about the state of the qubit and backaction dephasing of the system. The measurement effectiveness of the detector is characterized by the signal-to-noise ratio (SNR)

$$\text{SNR} = \frac{S(\Delta) - S_p}{S_p},$$

where $S_p = S(\omega \rightarrow \infty)$ is the pedestal of the noise spectrum. The SNR provides the measure of detector “ideality”, i.e., shows how close the detector can be quantum limited.

In the Markovian limit, there is a fundamental limit imposed on the SNR, i.e., equal to four, which is known as the Korotkov-Averin (K-A) bound [36]. This is a universal limit, independent of the coupling strength between the detector and system. In the presence of a strong non-Markovian effect as we discuss here, the resolvent of the kernel $\tilde{\Pi}_{\pm}(z)$ decays exponentially due to its finite-frequency-support feature, and approaches zero as $\omega \rightarrow \infty$. Thus the pedestal of the noise is completely suppressed, which results in a strong enhancement of the SNR, and eventually leads to a drastic violation of the K-A bound. Physically, the finite-frequency-support characteristics restrict the channels for electrons to transfer between the QPC reservoirs, which is accompanied by the energy $\hbar\omega$ absorption and emission of detection.

The bandwidth of the QPC detector is another essential quantity that can influence the non-Markovian dynamics. For a narrow bandwidth, the channels that electron can transfer between the QPC reservoirs are very limited, thus the non-Markovian effects on the qubit dynamics are suppressed, which results in prominent resonant peaks, particularly at large measurement voltage, as shown by the solid curve in Fig. 2(b). An decrease in the measurement voltage enhances non-Markovian dynamics, and thus suppress resonant peak, see the solid curve in Fig. 2(a). More channels open whenever the bandwidth increase. It leads to a growing non-Markovian

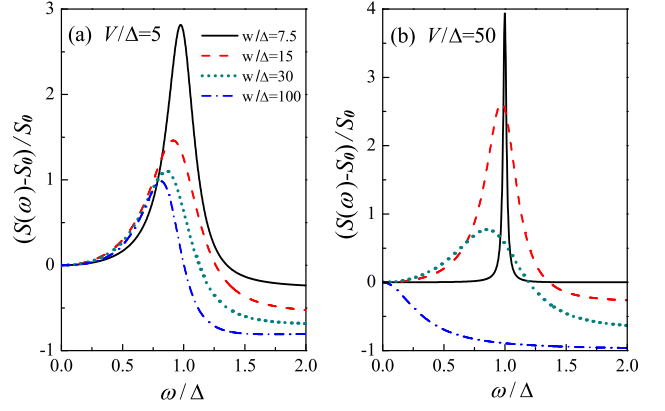


FIG. 2: Noise feature for a symmetric qubit ($\epsilon = 0$) for various bandwidths (w) at measurement voltages (a) $V/\Delta = 5$ and (b) $V/\Delta = 50$. The temperature is $\beta\Delta = 1$. Other parameters are $\eta\Delta^2 = 2$, $\chi_a = 0.8\Delta$ and $\chi_b = 0.2\Delta$.

effect on the dynamics of the reduced system, which suppresses coherent tunneling between the two dots. As a result, the peak height is reduced and line broadens towards the lower frequencies, as illustrated in Fig. 2(a) and (b).

At low bias voltage, the coherent jumps cannot be destroyed completely even in the wideband limit, as we have verified numerically. However, for a large voltage and bandwidth, the resonant peak is completely smeared [cf. the dash-dotted curve in Fig. 2(b)], in contrast to the previous results that resonant peaks exists in the Markovian regime and wideband limit [37–39, 47]. In this regime, a strong non-Markovian effect attempts to localize the electron in one of the dots for a longer time, leading thus to a complete transition from coherent to incoherent electron jumps. This is a clear signature of quantum Zeno effect due to strong non-Markovian effect. Eventually, the oscillation line turns into a spectral peak at zero frequency.

The effect of temperature on the noise spectrum are displayed in Fig. 3, where complex relaxation and dephasing of the qubit are involved. As the temperature rises, there is a remarkable increase in the dephasing rate, which leads to a suppression and broadening of the resonance peak, as shown in Fig. 3(a) and (b), for narrow and broad bandwidths, respectively. For a sufficient large temperature (for instance, $k_B T = 10\Delta$), a large dephasing rate results in a strong freezing of qubit; however, finite qubit relaxation induced by inelastic tunneling in the QPC gives rise to a delocalization of the electron, and thus suppresses the telegraph noise peak near zero frequency. Nevertheless, the spontaneous relaxation discussed here does not completely destroy the incoherent peak, reflecting the survive of the Zeno effect [see the solid curve in Fig. 3(b)]. This is in contrast to Ref. [39], where the relaxation resulted in the disappearance of the Zeno effect.

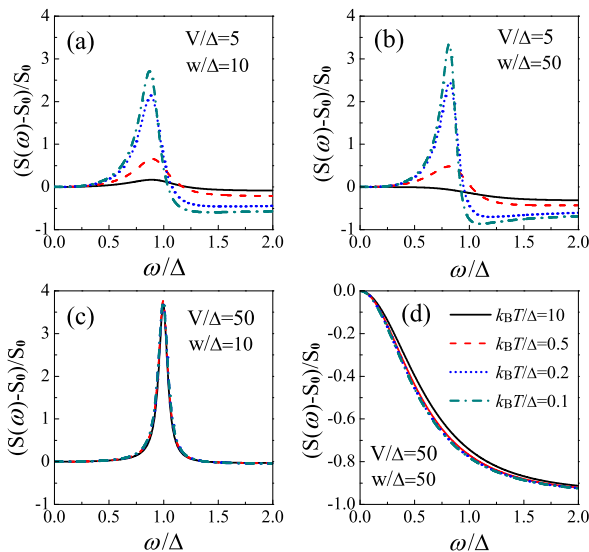


FIG. 3: Noise spectrum of a symmetric qubit at various temperatures for different voltages and bandwidths. The other parameters are the same as those in Fig. 2.

For a large measurement voltage and narrow bandwidth, the channels that electrons can pass through the QPC is markedly limited, due to large mismatch of the Fermi energies of the left and right QPC electrodes. In this regime, electron coherent jumps dominates, and the resonant peaks is robust against the temperature, as shown in Fig. 3(c). Unambiguously, this provides an effective way to manipulate coherent oscillations of a qubit under continuous measurement. An increase in bandwidth enhances non-Markovian effect, which tends to localize electron in one of the dots, leading thus to in-

coherent jumps, as indicated by zero-frequency peaks in Fig. 3(d). Strikingly, there is a complex balance between localization and delocalization due to qubit dephasing and spontaneous relaxation, respectively. Eventually it gives rise to a spectrum insensitive to the measurement temperature.

V. CONCLUSIONS

In summary, we have investigated the dynamics in continuous electric measurement of a charge qubit, with special attention paid to the non-Markovian measurement characteristics. The finite-frequency-support feature in the non-Markovian domain leads to a complete suppression of the noise pedestal, which causes a drastic violation of the Korotkov-Averin bound. For a large bandwidth and voltage ($w, V \gg \Delta$), strong non-Markovian correlations result in a coherent to incoherent transition, which diminishes the resonant peak in the spectrum. At a large voltage but narrow bandwidth, the electron coherent jumps remain robust over a wide range of temperatures, which could be utilized as an effective approach to manipulate coherent oscillations between two quantum states.

Acknowledgments

Support from the National Natural Science Foundation of China (10904128, 11004124, and 11147114), the Zhejiang Provincial Natural Science Foundation (Y6110467), and the Zhejiang University of Science and Technology (2011JC09Y) is gratefully acknowledged.

-
- [1] V. B. Braginsky and F. Y. Khalili, *Quantum Measurement* (Cambridge University Press, Cambridge, 1992).
 - [2] A. E. Allahverdyan, R. Balian, and T. M. Nieuwenhuizen, LANL e-print arXiv:1107.2138 (2011).
 - [3] A. Shnirman and G. Schön, Phys. Rev. B **57**, 15400 (1998).
 - [4] M. H. Devoret and R. J. Schoelkopf, Nature **406**, 1039 (2000).
 - [5] Y. Makhlin, G. Schön, and A. Shnirman, Rev. Mod. Phys. **73**, 357 (2001).
 - [6] A. A. Clerk, S. M. Girvin, A. K. Nguyen, and A. D. Stone, Phys. Rev. Lett. **89**, 176804 (2002).
 - [7] H. Jiao, X.-Q. Li, and J. Y. Luo, Phys. Rev. B **75**, 155333 (2007).
 - [8] T. Gilad and S. A. Gurvitz, Phys. Rev. Lett. **97**, 116806 (2006).
 - [9] S. A. Gurvitz and G. P. Berman, Phys. Rev. B **72**, 073303 (2005).
 - [10] N. P. Oxtoby, H. M. Wiseman, and H.-B. Sun, Phys. Rev. B **74**, 045328 (2006).
 - [11] E. Buks, R. Schuster, M. Heiblum, D. Mahalu, and V. Umansky, Nature **391**, 871 (1998).
 - [12] R. J. Schoelkopf, P. Wahlgren, A. A. Kozhevnikov, P. Delsing, and D. E. Prober, Science **280**, 1238 (1998).
 - [13] Y. Nakamura, Y. A. Pashkin, and J. S. Tsai, Nature (London) **398**, 786 (1999).
 - [14] D. Sprinzak, E. Buks, M. Heiblum, and H. Shtrikman, Phys. Rev. Lett. **84**, 5820 (2000).
 - [15] A. Aassime, G. Johansson, G. Wendin, R. J. Schoelkopf, and P. Delsing, Phys. Rev. Lett. **86**, 3376 (2001).
 - [16] Y. V. Nazarov, *Quantum Noise in Mesoscopic Physics* (Kluwer, Dordrecht, 2003).
 - [17] D. A. Rodrigues and A. D. Armour, New J. Phys. **7**, 251 (2005).
 - [18] D. Mozyrsky, I. Martin, and M. B. Hastings, Phys. Rev. Lett. **92**, 018303 (2004).
 - [19] A. A. Clerk and S. M. Girvin, Phys. Rev. B **70**, 121303 (2004).
 - [20] J. Wabnig, D. V. Khomitsky, J. Rammer, and A. L. Shelankov, Phys. Rev. B **72**, 165347 (2005).

- [21] H. S. Goan, G. J. Milburn, H. M. Wiseman, and H. B. Sun, Phys. Rev. B **63**, 125326 (2001).
- [22] A. N. Korotkov, Phys. Rev. B **63**, 115403 (2001).
- [23] T. M. Stace and S. D. Barrett, Phys. Rev. Lett. **92**, 136802 (2004).
- [24] C. Flindt, T. Novotný, and A.-P. Jauho, Phys. Rev. B **70**, 205334 (2004).
- [25] G. Kießlich, P. Samuelsson, A. Wacker, and E. Schöll, Phys. Rev. B **73**, 033312 (2006).
- [26] S.-K. Wang, H. Jiao, F. Li, X.-Q. Li, and Y. J. Yan, Phys. Rev. B **76**, 125416 (2007).
- [27] Z. Feng, J. Maciejko, J. Wang, and H. Guo, Phys. Rev. B **77**, 075302 (2008).
- [28] X. Zheng, J. Y. Luo, J. S. Jin, and Y. J. Yan, J. Chem. Phys. **130**, 124508 (2009).
- [29] P. Zedler, G. Schaller, G. Kiesslich, C. Emary, and T. Brandes, Phys. Rev. B **80**, 045309 (2009).
- [30] C. Flindt, T. Novotný, A. Braggio, M. Sassetti, and A.-P. Jauho, Phys. Rev. Lett. **100**, 150601 (2008).
- [31] R. Aguado and T. Brandes, Phys. Rev. Lett. **92**, 206601 (2004).
- [32] J. Jin, X.-Q. Li, M. Luo, and Y. J. Yan, J. Appl. Phys. **109**, 053704 (2011).
- [33] A. Braggio, J. König, and R. Fazio, Phys. Rev. Lett. **96**, 026805 (2006).
- [34] P.-W. Chen, C.-C. Jian, and H.-S. Goan, LANL e-print arXiv:1101.2393 (2011).
- [35] Y. J. Yan, Phys. Rev. A **58**, 2721 (1998).
- [36] A. N. Korotkov and D. V. Averin, Phys. Rev. B **64**, 165310 (2001).
- [37] A. Shnirman, D. Mozyrsky, and I. Martin, LANL e-print cond-mat/0211618 (2002).
- [38] J. Y. Luo, H. J. Jiao, F. Li, X.-Q. Li, and Y. J. Yan, J. Phys.: Cond. Matt. **21**, 385801 (2009).
- [39] S. A. Gurvitz, L. Fedichkin, D. Mozyrsky, and G. P. Berman, Phys. Rev. Lett. **91**, 066801 (2003).
- [40] R. X. Xu and Y. J. Yan, J. Chem. Phys. **116**, 9196 (2002).
- [41] Y. J. Yan and R. X. Xu, Annu. Rev. Phys. Chem. **56**, 187 (2005).
- [42] A. O. Caldeira and A. J. Leggett, Physica A **121**, 587 (1983).
- [43] U. Weiss, *Quantum Dissipative Systems* (World Scientific, Singapore, 2008), 3rd ed.
- [44] C. Meier and D. J. Tannor, J. Chem. Phys. **111**, 3365 (1999).
- [45] X. Q. Li and Y. J. Yan, Phys. Rev. B **75**, 075114 (2007).
- [46] D. K. C. MacDonald, *Noise and Fluctuations: An Introduction* (Wiley, New York, 1962), ch. 2.2.1.
- [47] S. A. Gurvitz, Phys. Rev. B **56**, 15215 (1997).